

# Three-dimensional "Mercedes-Benz" model for water

Cristiano L. Dias<sup>1,\*</sup>, Tapio Ala-Nissila<sup>2,3,†</sup>, Martin Grant<sup>4,‡</sup> and Mikko Karttunen<sup>1,§</sup>

<sup>1</sup>*Department of Applied Mathematics, The University of Western Ontario, London, Ontario, Canada N6A 5B7*

<sup>2</sup>*Department of Physics, Brown University, Providence RI 02912-1843*

<sup>3</sup>*COMP Center of Excellence and Department of Applied Physics, Helsinki University of Technology, P.O. Box 1100, FI-02015 TKK, Espoo, Finland*

<sup>4</sup>*Department of Physics, McGill University, 3600 rue University, Montréal, Québec, Canada H3A 2T8*

(Dated: February 13, 2009)

In this paper we introduce a three-dimensional version of the Mercedes-Benz model to describe water molecules. In this model van der Waals interactions and hydrogen bonds are given explicitly through a Lennard-Jones potential and a Gaussian orientation-dependent terms, respectively. At low temperature the model freezes forming Ice-I and it reproduces the main peaks of the experimental radial distribution function of water. In addition to these structural properties, the model also captures the thermodynamical anomalies of water: the anomalous density profile, the negative thermal expansivity, the large heat capacity and the minimum in the isothermal compressibility.

## I. INTRODUCTION

Water is the most important fluid on earth. It covers two thirds of the planet's surface and controls its climate. Most importantly, water is necessary for carbon-based organic life being the solvent in most *in vivo* chemical reactions. Its unique hydration properties drive biological macromolecules towards their three-dimensional structure, thus accounting for their function in living organisms [1]. Water exhibits anomalous properties that affect life at a larger scale. For example, mammals benefit from the large latent heat of water to cool them down through sweating, while water's large heat capacity prevents local temperature fluctuations, facilitating thermal regulation of organisms.

These anomalous properties result from a competition between isotropic van der Waals interactions and highly directional hydrogen bonding (H-bond). A large number of models of varying complexity have been developed and analyzed to model water's extraordinary properties, for reviews see e.g. Refs. [2, 3, 4, 5], but none of the current models can correctly reproduce all physical properties of water. Those model are typically calibrated against experimental data, for example the radial distribution function (RDF) at ambient conditions [6, 7], or the temperature of maximum density [8], i.e.  $T = 3.98^\circ\text{C}$ . While there is no guarantee that a model optimized to reproduce a given property is able to account for others, adding details increases its quantitative accuracy. For example, TIP5P, which describes water through 5 interacting sites, is typically more accurate [8] than models with 3 or 4 interacting sites. The addition of each interacting site, however, makes the model considerably much more demanding computationally. This is an undesirable feature

since a large number of water molecules is required to hydrate even the smallest peptides resulting in a high computational cost. Thus, simple models, such as SPC [9] and TIP3P [10, 11], are the most used ones in computational studies of biologically motivated systems. In addition, new models and improvements appear frequently in literature, see e.g., Refs. [12, 13, 14, 15] and references in them.

Coarse-grained models have also been developed and used to study the emergence of water's anomalous properties from its atomic constituents. Both lattice [16, 17, 18] and continuous models [19, 20, 21, 22] have been applied. Current coarse-grained models cannot, however, be easily used to study hydration of macromolecules, because they can not reproduce the structure of liquid water which is essential in studies of biological systems and molecules [1]. A proper structural description is required since hydration and, in particular, the hydrophobic effect, which is the main driving force for protein folding [23, 24], depend on the amount of structural order close to the hydrated molecule versus the amount of order in bulk water. A simplified model that would account for both thermodynamical and structural properties of water, would therefore be highly beneficial in studies related to the hydrophobic effect, protein folding and macromolecules in general.

The main purpose of this work is to introduce a simple but realistic model that reproduces both the main structural and thermodynamic properties of water. To this end, we extend the two dimensional (2D) Mercedes-Benz (MB) model [25] to 3D. In 2D, the MB model has already provided insights into several properties of water: its anomalous thermodynamical behavior [19], hydration of non-polar solutes [26], ion solvation [27], cold denaturation of proteins [28], and the properties of different amino acids [29]. Despite this success, there are several mechanisms which cannot be studied in two dimensions and an extension to 3D is needed.

We show that a previously proposed framework for the 3D MB model [30] does not reproduce the thermodynamical anomalies of water. Here, we extend the model to

\*Electronic address: diasc@physics.mcgill.ca

†Electronic address: Tapio.Ala-Nissila@tkk.fi

‡Electronic address: martin.grant@mcgill.ca

§Electronic address: mkarttu@uwo.ca

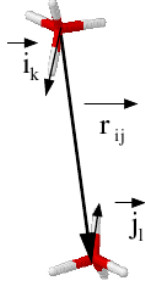


FIG. 1: (Color online) Schematic representation of two Mercedes-Benz molecules and important vectors defining their interaction.

overcome that problem by making H-bonding dependent on the local environment of atoms by penalizing compact configurations in favor of open-packed ones. With this implementation, structural and thermodynamical properties of are recovered qualitatively. We would like to emphasize that our goal is not to replace atomistically accurate models, such as TIP5P, but rather to provide an alternative for qualitative studies involving water.

The rest of this paper is organized as follows: next, we introduce and discuss the existing 3D MB model, and propose a correction that makes the model suitable to describe thermodynamical and structural properties of water. In the same section, we present the Monte-Carlo scheme and the cooling protocol used in this work. We present our results and comparison to experimental results in Sec. III. In the section entitled results, experimental data are compared qualitatively to our simulations. Finally, we present our conclusions and a discussion in Sec. IV.

## II. THE MODEL

### A. Mercedes Benz model

In the 3D MB model, water molecules interact explicitly through two types of empirical potentials: H-bonds and van der Waals. H-bonds are directional and account for the tetrahedral structure of water which is described by four arms separated from each other by angles of  $109.47^\circ$ , see Fig. 1. The energy of H-bonds is minimized whenever arms of adjacent molecules point towards each other. Mathematically if  $\vec{X}_i$  represents the position of the  $i^{\text{th}}$  particle and its four unitary arms, which are denoted by  $\vec{i}_k$  (with  $k = 1, 2, 3, 4$ ), then H-bond interaction between molecules  $i$  and  $j$  can be written as

$$U_{HB}(\vec{X}_i, \vec{X}_j) = \sum_{k,l=1}^4 U_{HB}^{kl}(r_{ij}, \vec{i}_k, \vec{j}_l), \quad (1)$$

where

$$U_{HB}^{kl}(r_{ij}, \vec{i}_k, \vec{j}_l) = \epsilon_{HB} G(r_{ij} - R_{HB}, \sigma_R) \times G(\vec{i}_k \hat{r}_{ij} - 1, \sigma_\theta) G(\vec{j}_l \hat{r}_{ij} - 1, \sigma_\theta) \quad (2)$$

and  $G(x, \sigma)$  is an unnormalized Gaussian function

$$G(x, \sigma) = \exp[-x^2/2\sigma^2]. \quad (3)$$

The above mathematical description ensures that the intensity of a H-bond is maximized whenever the arms of neighboring molecules are aligned with the vector  $\vec{r}_{ij}$  joining their centers of mass and whenever their distance is equal to  $R_{HB}$ .

The spherically symmetric van der Waals interactions are approximated by a Lennard-Jones potential:

$$U_{LJ}(r_{ij}) = 4\epsilon_{LJ} \left[ \left( \frac{\sigma_{LJ}}{r_{ij}} \right)^{12} - \left( \frac{\sigma_{LJ}}{r_{ij}} \right)^6 \right], \quad (4)$$

where  $\epsilon_{LJ}$  describes the strength of the interaction and  $\sigma_{LJ}$  is the particle diameter. Then, the total energy describing two MB particles is given by

$$U(\vec{X}_i, \vec{X}_j) = U_{LJ}(r_{ij}) + U_{HB}(\vec{X}_i, \vec{X}_j). \quad (5)$$

Bizjak *et al.* [30] studied this model using the following set of parameters:  $\epsilon_{HB} = -1$ ,  $\epsilon_{LJ} = 1/35\epsilon_{HB}$ ,  $R_{HB} = 1$ ,  $\sigma_{LJ} = 0.7$ ,  $\sigma_R = \sigma_\theta = 0.085$ . They assumed a diamond structure for the model's ground state which is the configuration taken by oxygen atoms when water forms cubic ice, i.e. Ice-I<sub>c</sub>. When tested against simulation, however, this assumption fails and the model can be shown to minimize its energy in an Ice-VII configuration: two interpenetrating diamond lattices with no H-bonds connecting these lattices.

Ice-VII appears to be the optimized ground state for systems trying to maximize their density within a tetrahedral symmetry. It is therefore natural that the 3D MB model of Bizjak *et al.* [30], whose H-bond term imposes a tetrahedral configuration and the van der Waals term favors compact conformations, has this structure as its ground state. However Ice-VII is not the desired ground state for models of water at ambient pressure such that 3D lattice models for this material have an explicit energetic term penalizing compact configurations of this type [18, 31, 32].

Figure 2(a) shows a typical Ice-VII ground state obtained by quenching a system of 256 MB particles interacting through the framework of Bizjak *et al.*. Details about the simulation method and the cooling procedure will be described later in this section. Figure 2(b) shows the density obtained along quenching. The liquid phase has a higher density than ice – as in real water. However, the model does not reproduce the density anomaly of water: the liquid phase does not show a temperature of maximum density below which the density decreases. As a result, the thermal expansion coefficient is never found to be negative in the liquid phase (Fig. 2(b)). In

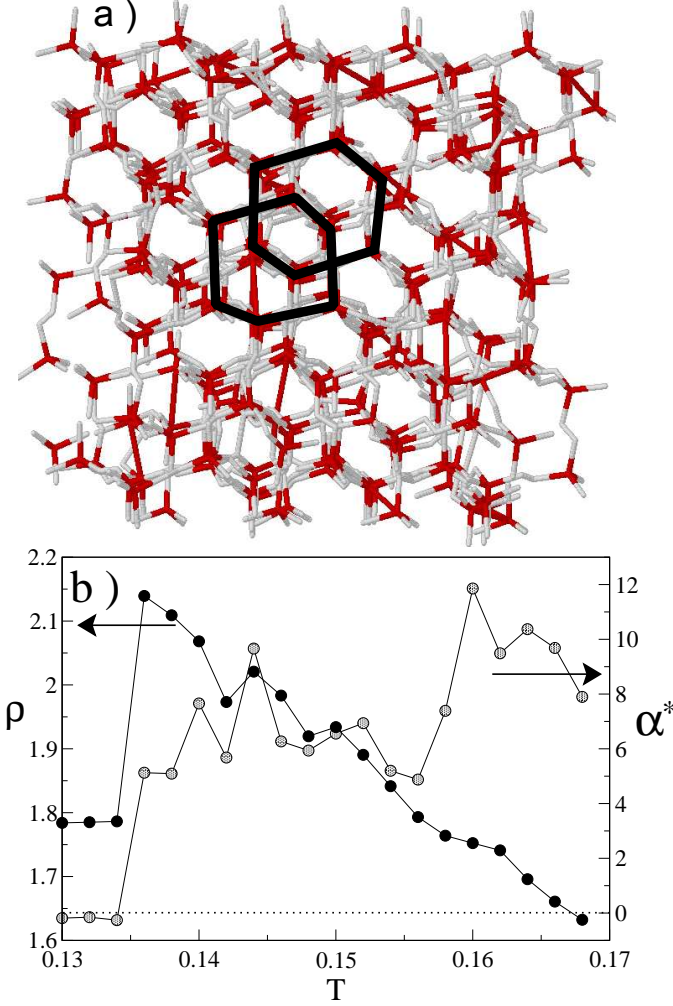


FIG. 2: (Color online) (a) Ground state of the Mercedes-Benz model: Ice-VII. As a guide to the eye two hexagons, representing the two interpenetrating diamond structure of ice-VII, are drawn. (b – left axis) Dependence of the density ( $\text{g}/\text{cm}^3$ ) on temperature (in units of  $\epsilon_{HB}$ ). (b – right axis) Dependence of the coefficient of thermal expansion ( $\epsilon_{HB}^{-1}$ ) on temperature. A constant pressure of 0.2 in units of  $\epsilon_{HB}/R_{HB}^3$  was used.

addition, the model does not reproduce the structure of liquid water (see Fig. 3 in Ref. [30]): the simulated RDF has a non-realistic peak at a distance corresponding to the van der Waals radius.

Despite the problems cited above, the 3D MB model remains an attractive coarse-grained model for water. It does not require calculation of charges, which enables longer simulation times desperately needed in studies of macromolecules. It also holds the promise of being able to provide a qualitatively accurate description of the structure of water due to its tetrahedral nature [33] and water's thermodynamical properties since the model exhibits both open and close packed structures required to describe water's anomalous behavior [20]. Next, we de-

scribe how the model of Bizjak *et al.* [30] can be improved to better describe the structure and thermodynamics of water.

### B. Corrections to the Mercedes-Benz model

To resolve the above problems, we introduce a term that depends on the local environment of particles. Our approach is inspired by Tersoff-like potentials for covalent materials [34]. This term penalizes H-bonds which are formed in crowded environments through the factor

$$b(z_i) = \begin{cases} 1, & \text{if } z_i \leq 4 \\ \left(\frac{4}{z_i}\right)^v, & \text{if } z_i > 4, \end{cases} \quad (6)$$

where  $z_i$  is the coordination of atom  $i$ , computed as  $z_i = \sum_{k \neq i} f(r_{ik})$  with the cut-off function defined by [34]:

$$f(r_{ij}) = \begin{cases} 1, & r < R - D \\ \frac{1}{2} - \frac{1}{2} \sin\left(\frac{\pi}{2}(r - R)/D\right), & R - D < r < R + D \\ 0, & r > R + D \end{cases} \quad (7)$$

where  $R$  and  $D$  are chosen as to include the first-neighbor shell only. Note that  $f(r)$  decreases continuously from 1 to 0 in the range  $R - D < r < R + D$ .

The energy of H-bonds corrected through Eq. (6) becomes:

$$U_{HB}^c(\vec{X}_i, \vec{X}_j) = b(z_i) \sum_{k,l=1}^4 U_{HB}^{kl}(r_{ij}, \vec{i}_k, \vec{j}_l). \quad (8)$$

This equation penalizes H-bonds whenever interacting molecules have more than four neighbors. This inhibits the formation of compact tetrahedral phases, e.g. Ice-VII, and favors open-packed tetrahedral phases such as Ice-I.

In order to ensure that H-bonds favor chair-like configurations required for diamond structure, we also add a standard potential with three-fold symmetry for dihedral angles. This potential adds an energetic cost to the H-bond between arms  $m$  of molecule  $i$  and arm  $n$  of molecules  $j$ , if the dihedral angle formed by the other arms of these molecules is not  $60^\circ$ :

$$U_\phi^{mn}(\vec{X}_i, \vec{X}_j) = \frac{\epsilon_\phi}{2} U_{HB}^{mn}(r_{ij}, \vec{i}_m, \vec{j}_n) b(z_i) \times \sum_{\substack{k \neq m \\ l \neq n}} (1 + \cos(3\phi_{kl})), \quad (9)$$

where  $\epsilon_\phi$  is the strength of the interaction. The term  $U_{HB}^{mn}(r_{ij}, \vec{i}_m, \vec{j}_n) b(z_i)$  ensures that the penalty is proportional to the strength of the H-bond. The dihedral angle  $\phi_{kl}$  describes how the arm  $k$  of molecule  $i$  aligns with the arm  $l$  of molecule  $j$  along the vector joining the center

of mass of these two molecules. Thus, the total dihedral energy between molecules  $i$  and  $j$  is

$$U_\phi(\vec{X}_i, \vec{X}_j) = \sum_{m,n} U_\phi^{mn}(\vec{X}_i, \vec{X}_j). \quad (10)$$

Note that because of the dependence on the local environment,  $U_{HB}^c(\vec{X}_i, \vec{X}_j) \neq U_{HB}^c(\vec{X}_j, \vec{X}_i)$  and  $U_\phi^{mn}(\vec{X}_i, \vec{X}_j) \neq U_\phi^{nm}(\vec{X}_j, \vec{X}_i)$ . This asymmetry has no physical implications since  $U_{HB}^c$  and  $U_\phi$  possess all the invariance properties required for a potential [34].

We can now write the total potential energy between two water molecules as

$$E(\vec{X}_i, \vec{X}_j) = U_{LJ}(r_{ij}) + U_{HB}^c(\vec{X}_i, \vec{X}_j) + U_\phi(\vec{X}_i, \vec{X}_j). \quad (11)$$

This model has 10 parameters which were chosen such as to account for a semi-quantitative agreement of the density profile with experiment. We proceeded in two steps to adjust these parameters. First, we chose the values for these parameters such as to produce a density in  $\text{g/cm}^3$  [37] that is comparable to experimental values, i.e. about  $1 \text{ g/cm}^3$  for the liquid phase and  $0.93 \text{ g/cm}^3$  for the ice phase. Only under this condition can the structure of the model be qualitatively similar to real water. Then, we adjusted the parameters such as to obtain a density that is a concave function of temperature with its maximum close to the freezing point. This second condition is the minimal requirement for describing the anomalous properties of water.

The set of parameters calibrated according to the above procedure is given here in reduced units. We report energies and distances in terms of the binding energy  $|\epsilon_{HB}|$  and equilibrium distance  $R_{HB}$  of the H-bond. In these units, the three binding energies describing the system are  $\epsilon_{HB} = -1$ ,  $\epsilon_{LJ} = 0.05$  and  $\epsilon_\phi = 0.01$ . The two distances are  $R_{HB} = 1$  and  $\sigma_{LJ} = 1.04/2^{1/6}$ . The two terms controlling H-bond interaction are  $\sigma_R = 0.1$  and  $\sigma_\theta = 0.08$ , and the three parameters controlling the penalty of crowded environments are  $v = 0.5$ ,  $R = 1.3$  and  $D = 0.2$ . In this work, temperature is given in units of  $|\epsilon_{HB}|/k_B$ , where Boltzmann's constant  $k_B$  is set to unity. Pressure is given in units of  $|\epsilon_{HB}|/R_{HB}^3$ .

While adjusting the parameters, we found that the behavior of the system is robust upon changing the variables characterizing crowded environments. It is, however, sensitive to the ratio between the binding energy of the van der Waals interaction and the binding energy of the H-bond. This ratio controls the interplay of forces leading to an environment where MB molecules are radially surrounded by their first-neighbors, and forces favoring a tetrahedral distribution of the first-neighbors. The latter favors a high density configuration while the former accounts for a low density one. As opposed to the 2D MB model, we kept the equilibrium distance of the van der Waals interaction comparable to the equilibrium distance of the H-bond such as to avoid artificial peaks in the RDF [30].

### C. Numerical simulation method

For numerical simulations, we use the isothermal-isobaric (NPT) ensemble to study the thermodynamical properties of a system made of  $N = 256$  MB particles. A Monte-Carlo scheme is used where, at each step, an attempt is made to displace the center of mass and the orientation of particles randomly by a quantity  $\Delta R_{max}$  and  $0.125$  rad, respectively. The maximum translational displacement is chosen such as to give an acceptance ratio of 50%. Periodic boundary conditions are used to mimic an infinite system and at every 5 Monte Carlo sweeps, an attempt to rescale the size of the box is made (1 Monte Carlo sweep is equivalent to  $N$  attempted steps).

To obtain thermodynamical data throughout the desired range of temperatures, the initial configuration of the system is chosen randomly and equilibrated at the highest temperature ( $T = 0.17$ ) for  $5 \times 10^4$  sweeps, after which statistics are gathered for the same amount of time. Then, the system is cooled down by  $\Delta T = 0.002$  and a similar cycle of equilibration/data gathering is performed. This cooling procedure is repeated until the lowest temperature, i.e.  $T = 0.11$  is reached. At the transition temperature an additional cycle of equilibration/statistics gathering ensured that the system was equilibrated properly. For all the pressures studied here, this protocol was repeated for 10 samples differing by the initial condition. All the quantities reported are the average over those 10 samples and, whenever relevant, the root-mean-square of this average is also shown as the error-bar.

The quantities computed during the simulations were the average potential energy per particle  $E$ , the volume per particle  $V$ , the heat capacity  $C_P$ , the compressibility  $\kappa_T$  and the thermal expansion coefficient  $\alpha_P$ . The last three quantities are computed mathematically from the standard fluctuation relations:

$$\begin{aligned} C_P^* &= \frac{C_P}{k_B} = \frac{\langle H^2 \rangle - \langle H \rangle^2}{NT^2}, \\ \kappa_T^* &= \frac{\langle V^2 \rangle - \langle V \rangle^2}{T\langle V \rangle}, \\ \alpha_P^* &= \frac{\langle VH \rangle - \langle V \rangle \langle H \rangle}{T^2 \langle V \rangle}, \end{aligned} \quad (12)$$

where  $H$  corresponds to the enthalpy of the system. As for the other quantities computed during the simulation, these response functions will be given in reduced units. Thus,  $C_P^*$  will be reported in dimensionless units,  $\kappa_T^*$  in terms of  $R_{HB}^3/\epsilon_{HB}$  and  $\alpha_P^*$  in units of  $\epsilon_{HB}^{-1}$ .

### III. RESULTS

In Fig. 3, we provide a qualitative comparison between the properties of bulk water (left panels) and the MB model at  $P = 0.2$  (right panels). The behavior of the

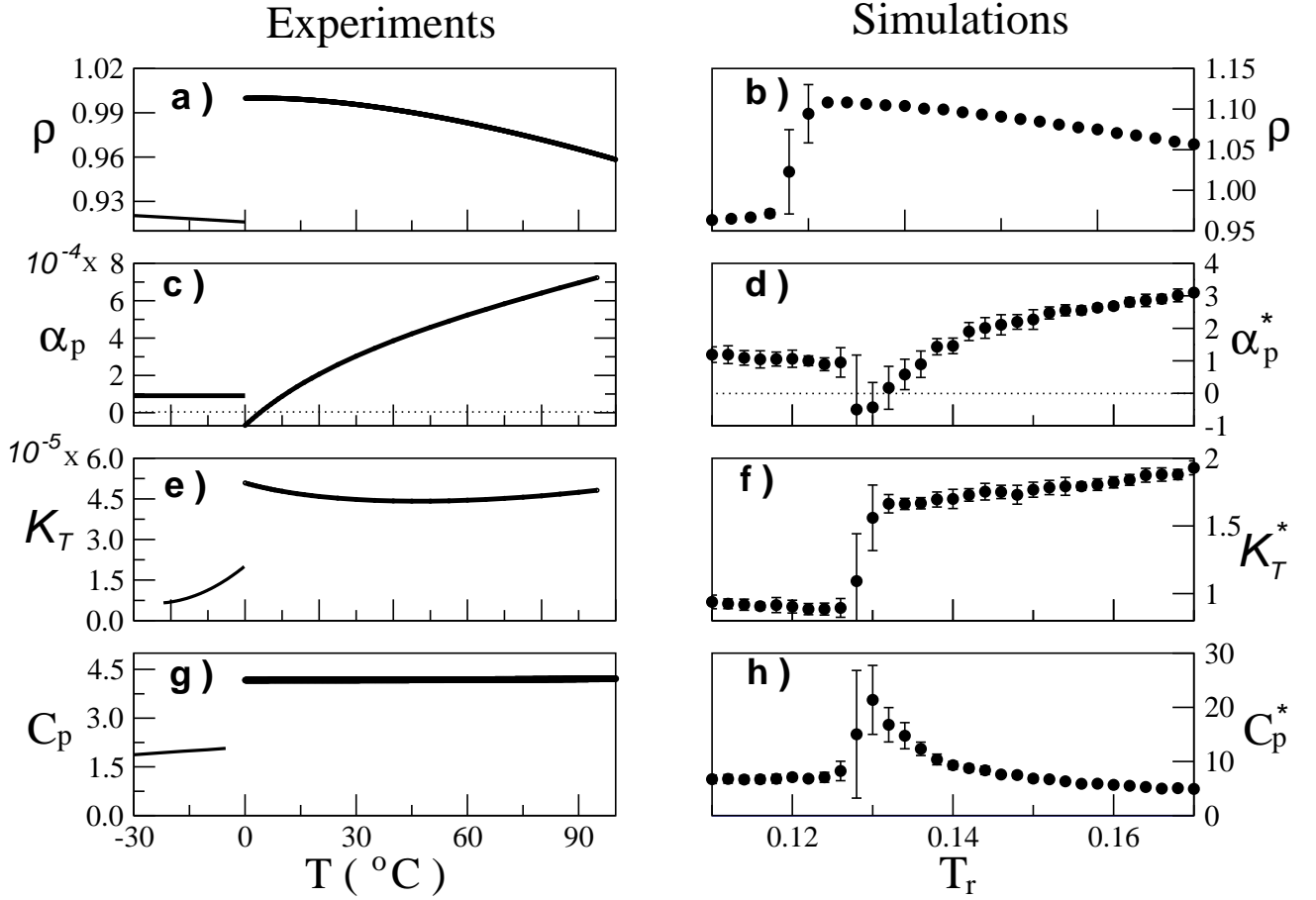


FIG. 3: Thermodynamical properties of water. *Left*: Experiments – data obtained from references [35]. Units are:  $\rho$  (g/cm<sup>3</sup>),  $\alpha_P$  (K<sup>-1</sup>),  $C_P$  (J / g / K) and  $\kappa_T$  (bar<sup>-1</sup>). *Right*: Simulations. Units are:  $\alpha_P^*$  ( $\epsilon_{HB}^{-1}$ ),  $\kappa_T^*$  ( $R_{HB}^3/\epsilon_{HB}$ ) and  $C_P^*$  (dimensionless units).

MB model follows the trends of water quite accurately: the anomalous density profile (panels on the first row), the negative thermal expansivity (second row), the minimum in the isothermal compressibility (third row) and the large heat capacity (fourth row).

At ambient pressure, water freezes into an open packed configuration called hexagonal-ice, i.e. Ice-I<sub>h</sub>. This structure is held together by H-bonds which break when ice melts. At this transition, water molecules fill part of the empty spaces, assuming a higher density. In the liquid phase close to the melting temperature, a few open-packed configurations persist – held together by H-bonds. As the system is heated up, those bonds melt gradually removing empty spaces and increasing the density of the system. This reduction of empty spaces occurs until the temperature of maximum density is reached. At this point thermal fluctuations decrease the density of the system with increasing temperature. This behavior has been measured experimentally (Fig. 3(a)) and is captured by the MB model (Fig. 3(b)): abrupt increase of the density at the melting transition and concave temperature dependence for the density of water with a maximum close to the melting transition.

The thermal expansion coefficient is proportional to the derivative of the volume with respect to temperature  $\alpha_P = 1/V(\partial V/\partial T)_P$ . As for most materials,  $\alpha_P$  decreases upon cooling (Fig. 3(c)) – indicating that the volume of water decreases with temperature. It becomes zero at the temperature of maximum density and negative close to the freezing point. This unusual negative expansivity is reproduced in the model (Fig. 3(d)) and reflects the unusual behavior of water to expand upon cooling below the temperature of maximum density.

The isothermal compressibility measures the tendency of a system to change its volume when the applied pressure is varied:  $\kappa_T = -1/V(\partial V/\partial P)_T$ . For a typical material,  $\kappa_T$  decreases upon cooling since it is related to density fluctuations whose amplitude becomes smaller as temperature decreases. This is in contrast with the behavior of water (Fig. 3(e)). The compressibility of water is a convex function of temperature and has a minimum. This anomalous behavior can be explained by noticing that the compressibility is lower for highly packed system than for loosely packed ones since highly packed systems are less susceptible to rearrange their conformation when subjected to a pressure change. Thus,  $\kappa_T$  correlates with



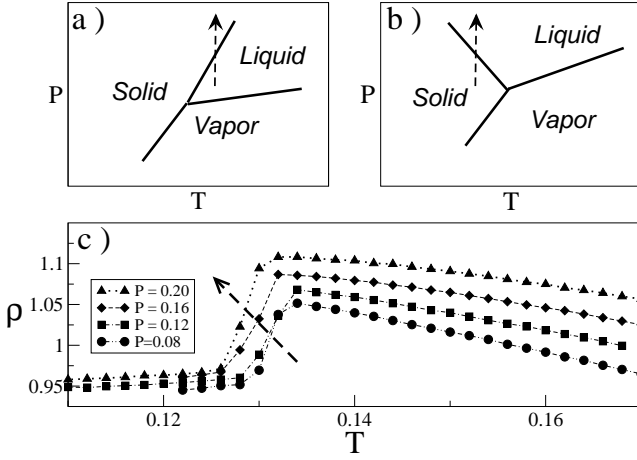


FIG. 4: Schematic representation of the phase diagram of a simple one-component substance (a) and water (b). Arrows indicate that pressure freezes a typical liquid but pressure melts ice. (c) Simulated density of the model for different values of pressure. Arrow indicates the shift of the freezing temperature to lower values as pressure increases.

the volume of the system [19]. Now, since the volume of water is a convex function of temperature,  $\kappa_T$  is also convex with respect to temperature for water – see Fig. 3(e). Fig. 3(f) shows that the simulated compressibility is also a convex function of temperature, although the curvature is not very pronounced and its minimum is not as pronounced as in experiments.

Heat capacity, which measures the capacity of a system to store thermal energy ( $C_P = (dH/dT)_P$ ), is much higher in water than in ice – see Fig. 3(h). This has been explained by the multiple energy storage mechanisms of water as the breakage of van der Waals interactions and H-bonds. The heat capacity of the model presents a much higher variability than real water: close to the transition,  $C_P$  is much higher than ice and this quantity decreases fast, reaching the same value as ice at about  $T = 0.15$ .

In Fig. 4(a), we illustrate schematically the coexistence lines of the solid, liquid and vapor phases of a simple material. At any point along those lines, the free energies of the adjacent phases are equivalent and the Clausius-Clapeyron equation is obtained by equating them:

$$\left(\frac{dP}{dT}\right)_{coex} = \frac{\Delta h}{T\Delta v}. \quad (13)$$

Since  $\Delta h < 0$  and  $\Delta v < 0$  for the liquid to solid transition of typical materials,  $(dP/dT)_{coex}$  is positive. As a result of this positive slope, a typical liquid freezes when pressure is applied to it – as illustrated by the arrow on Fig. 4(a). On the other side, since water expands upon freezing,  $\Delta v > 0$  while the enthalpy difference remains negative (ice has a lower enthalpy compared to water). Thus the coexistence line of the liquid-solid transition has a negative slope, i.e.  $(dP/dT)_{coex} < 0$ . This is illustrated in Fig. 4(b) and leads to the melting of ice when pressure is applied to it. In Fig. 4(c) we show that the model

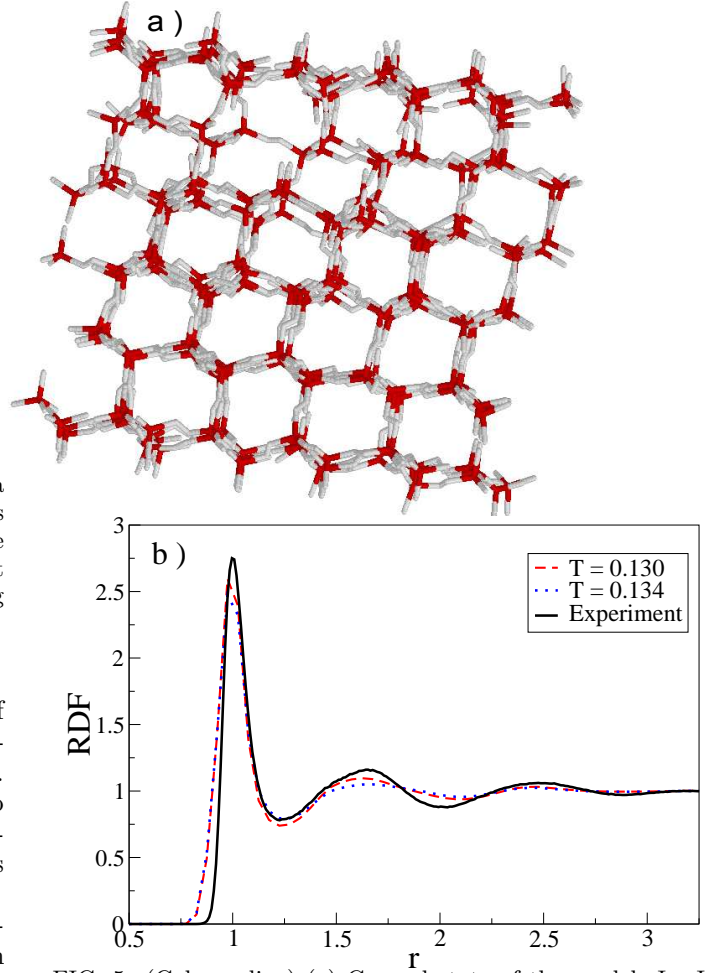


FIG. 5: (Color online) (a) Ground state of the model: Ice-I where oxygen atoms occupy positions on a diamond-like lattice. (b) Radial distribution function of the model at different temperatures compared to experimental data of water at 298 K.

reproduces this anomalous behavior of water. The simulated dependence of the density on temperature is shown for different values of pressure. The freezing temperature shifts to lower values as pressure increases, implying  $(dP/dT)_{coex} < 0$ .

Figure 5(a) shows the structure obtained by freezing the MB model. In this configuration, the center of a MB molecule occupies the sites of a diamond-like structure and its arms point to its four neighbors. Note that without a penalty term (Eq. (6)) the empty spaces found in Ice-I can be the stage for the formation of another tetrahedral-like lattice. Thus, this term efficiently shifts the energy of those compact configurations and, in particular Ice-VII, in favor of Ice-I. In Fig. 5(b), the experimental RDF [7] is compared to the ones of the model at different temperature. The second peak of the RDF, commonly referred to as tetrahedral peak [36], is a fingerprint of the tetrahedral geometry of water. It occurs at a distance given by the cosine rule,  $d^2 = 2R_{HB}^2 - 2R_{HB} \cos(109.4^\circ) \approx 1.6$ , much smaller than

for a simple liquid [36]. When compared to experiment, the model's RDF has slightly less structure but it peaks at the same position as the experiment – indicating that the average structure of the model agrees well with the experiment.

#### IV. CONCLUSION

In this work, we have constructed a simple but realistic model for water based on the Mercedes-Benz approach [19]. At low temperature the model freezes forming Ice-I and it reproduces the main peaks of the experimental RDF of bulk water. In addition to these structural properties, the model reproduces the density anomaly of water: ice has a lower density than water and the density of water is a concave function of temperature, with a maximum close to the freezing point. Also, the slope of the solid-liquid coexistence curve is also found to be negative, in agreement with experiments.

In the 2D MB model, the H-bond interaction favors environments having 3 first-neighbors at a distance  $R_{HB}$  which competes with the van der Waals interaction that favors 6 neighbors at a distance  $0.7R_{HB}$ . This competition is the underlying physics of the model that accounts for the density anomaly of bulk water. In the 3D MB model, H-bond and van der Waals interactions have the same equilibrium distance and the density anomaly re-

sults from an energy penalty for crowded environments. Without this penalty, the system would solidify into a compact Ice-VII configuration. With the penalty term, Ice-VII conformations compete with an open packed diamond-like structure. The competition between these interactions is the underlying mechanism that leads to the density anomaly of the system.

The MB model for water is based on local interactions which are much faster to compute than usual models that uses long-range Coulomb forces. We believe that this model will provide new insights into water mechanisms related to molecular hydration. In particular, investigations of the hydrophobic effect are being undertaken with this model.

#### Acknowledgements

C.L.D. would like to thank Razvan Nistor and Marco Aurelio Alves Barbosa for insightful discussions. He would also like to thank Alvarro Ferraz Filho and Silvio Quezado for kindly hosting his stay at the International Centre of Condensed Matter Physics (ICCP) in Brasilia, Brazil, where part of this work was completed. We would like to thank SharcNet ([www.sharcnet.ca](http://www.sharcnet.ca)) for computing resources. M.K. has been supported by NSERC of Canada and T.A.N. by the Academy of Finland through its COMP CoE and TransPoly grants.

- 
- [1] Martin Chaplin. Do we underestimate the importance of water in cell biology? *Nature Reviews Molecular Cell Biology*, 7(11):861–866, September 2006.
  - [2] William L. Jorgensen, Jayaraman Chandrasekhar, Jeffrey D. Madura, Roger W. Impey, and Michael L. Klein. Comparison of simple potential functions for simulating liquid water. *The Journal of Chemical Physics*, 79(2):926–935, 1983.
  - [3] I. Nezbeda. Simple short-ranged models of water and their application. a review. *Journal of Molecular Liquids*, 73-74:317–336, November 1997.
  - [4] Bertrand Guillot. A reappraisal of what we have learnt during three decades of computer simulations on water. *Journal of Molecular Liquids*, 101(1-3):219–260, November 2002.
  - [5] M. M. Conde C. Vega, J. L. F. Abascal and J. L. Aragones. What ice can teach us about water interactions: a critical comparison of the performance of different water models. *Faraday Discuss.*, 141:251, 2009.
  - [6] Jon M. Sorenson, Greg Hura, Robert M. Glaeser, and Teresa Head-Gordon. What can x-ray scattering tell us about the radial distribution functions of water? *J. Chem. Phys.*, 113:9149, 2000.
  - [7] A. K. Soper. The radial distribution functions of water and ice from 220 to 673 k and at pressures up to 400 mpa. *Chemical Physics*, Volume 258:121–137, 2000.
  - [8] Michael W. Mahoney and William L. Jorgensen. A five-site model for liquid water and the reproduction of the density anomaly by rigid, nonpolarizable potential functions. *J. Chem. Phys.*, 112:8910, 2000.
  - [9] H. J. C. Berendsen, J. P. M. Postma, W. F. van Gunsteren, and J. Hermans. Interaction models for water in relation to protein hydration. In B. Pullman, editor, *Intermolecular Forces*, pages 331–342. Reidel, Dordrecht, 1981.
  - [10] W. L. Jorgensen, J. Chandrasekhar, J. D. Madura, R. W. Impey, and M. L. Klein. Comparison of simple potential functions for simulating liquid water. *J. Chem. Phys.*, 79:926–935, 1983.
  - [11] Eyal Neria, Stefan Fischer, and Martin Karplus. Simulation of activation free energies in molecular systems. *J. Chem. Phys.*, 105:1902–1921, 1996.
  - [12] Daniel J. Price and Brooks. A modified tip3p water potential for simulation with ewald summation. *The Journal of Chemical Physics*, 121(20):10096–10103, 2004.
  - [13] Hans W. Horn, William C. Swope, Jed W. Pitera, Jeffrey D. Madura, Thomas J. Dick, Greg L. Hura, and Teresa Head-Gordon. Development of an improved four-site water model for biomolecular simulations: Tip4p-ew. *The Journal of Chemical Physics*, 120(20):9665–9678, 2004.
  - [14] Yujie Wu, Harald L. Tepper, and Gregory A. Voth. Flexible simple point-charge water model with improved liquid-state properties. *The Journal of Chemical Physics*, 124(2), 2006.
  - [15] András Baranyai and Albert Bartók. Classical interaction model for the water molecule. *The Journal of Chemical Physics*, 126(18), 2007.

- [16] Marco Aurlio Alves Barbosa and Vera Bohomoletz Henriques. Frustration and anomalous behavior in the bell-lavis model of liquid water. *Phys. Rev. E* 77, 051204 (2008), 77:51204, 2008.
- [17] C. Buzano, E. De Stefanis, A. Pelizzola, and M. Pretti. Two-dimensional lattice-fluid model with waterlike anomalies. *Phys. Rev. E*, 69:61502, 2004.
- [18] M. Pretti and C. Buzano. Thermodynamic anomalies in a lattice model of water: Solvation properties. *J. Chem. Phys.*, 123:24506, 2005.
- [19] Kevin A. T. Silverstein, A. D. J. Haymet, and Ken A. Dill. A simple model of water and the hydrophobic effect. *J. Am. Chem. Soc.*, 120 (13):3166–3175, 1998.
- [20] Peter H. Poole, Francesco Sciortino, Tor Grande, H. Eugene Stanley, and C. Austen Angell. Effect of hydrogen bonds on the thermodynamic behavior of liquid water. *Phys. Rev. Lett.*, 73:1632–1635, 1994.
- [21] A. P. Lyubartsev and A. Laaksonen. Determination of effective pair potentials from *ab-initio* simulations: Application to liquid water. *Chem. Phys. Lett.*, 325:15–21, 2000.
- [22] A. P. Lyubartsev, M. Karttunen, I. Vattulainen, and A. Laaksonen. On coarse-graining by the Inverse Monte Carlo method: Dissipative particle dynamics simulations made to a precise tool in soft matter modeling. *Soft Materials*, 1:121–137, 2003.
- [23] W. Kauzmann. *Adv. Protein Chem.*, 14:1, 1959.
- [24] Ken A. Dill. Dominant forces in protein folding. *Biochemistry*, 29:7133, 1990.
- [25] A. Ben-Naim. Statistical mechanics of "waterlike" particles in two dimensions. i. physical model and application of the percus yeveck equation. *The Journal of Chemical Physics*, 54:3682, 1971.
- [26] Noel T. Southall and Ken A. Dill. Potential of mean force between two hydrophobic solutes in water. *Biophysical Chemistry*, 101-102:295–307, 2002.
- [27] Ken A. Dill, Thomas M. Truskett, Vojko Vlachy, and Barbara Hribar-Lee. Modeling water, the hydrophobic effect, and ion solvation. *Annual Review of Biophysics and Biomolecular Structure*, 34:173, 2005.
- [28] Cristiano L. Dias, Tapio Ala-Nissila, Mikko Karttunen, Ilpo Vattulainen, and Martin Grant. Microscopic mechanism for cold denaturation. *Physical Review Letters*, 100:118101, 2008.
- [29] Jean-Paul Becker and Olivier Collet. Mercedes benz model of neutral amino-acid side chains. *Journal of Molecular Structure: THEOCHEM*, 774:23–28, 2006.
- [30] A. Bizjak, T. Urbic, V. Vlachy, and K.A. Dill. The three-dimensional "mercedes benz" model of water. *Acta Chimica Slovenica*, 54:532–537, 2007.
- [31] C. J. Roberts and Pablo G. Debenedetti. Polyamorphism and density anomalies in network-forming fluids: Zeroth- and first-order approximations. *J. Chem. Phys.*, 105:658, 1996.
- [32] G M Bell. Statistical mechanics of water: lattice model with directed bonding. *J. Phys. C: Solid State Phys*, 5:889, 1972.
- [33] J. D. Bernal and R. H. Fowler. A theory of water and ionic solution, with particular reference to hydrogen and hydroxyl ions. *J. Chem. Phys.*, 1:515, 1933.
- [34] J. Tersoff. New empirical approach for the structure and energy of covalent systems. *Phys. Rev. B*, 37:6991–7000, 1988.
- [35] GS Kell. Density, thermal expansivity, and compressibility of liquid water from 0. deg. to 150. deg.: Correlations and tables for atmospheric pressure and saturation reviewed and expressed on 1968 temperature scale. *Journal of Chemical and Engineering Data*, 20:97, 1975.
- [36] John L. Finney. The water molecule and its interactions: the interaction between theory, modelling, and experiment. *Journal of Molecular Liquids*, 90:303–312, 2001.
- [37] The density can be computed in g per cm<sup>3</sup> by mapping  $R_{HB}$  to its experimental value [7], i.e.  $R_{HB} = 2.78 \text{ \AA}$ , and using  $M = 2.992 \cdot 10^{-23} \text{ g}$  for the molecular mass of water:  $\rho = \left(\frac{256}{V}\right) 1.45448 \text{ g/cm}^3$ .